

4 Surface/Interface Project -Crystalline, magnetic and electronic structures at the surface and interface of magnetic thin films and multilayers-

Project Leader: Kenta Amemiya

4-1 Introduction

The surface and interface of magnetic thin films play essential roles in the appearance of extraordinary magnetic properties such as the perpendicular magnetic anisotropy and the giant magnetoresistance effect. We are investigating the crystalline, magnetic and electronic structures of the surface and interface of magnetic thin films and multilayers, in order to reveal the origin of the fascinating magnetic properties, which do not appear in bulk materials. We have studied, for example, Au/Co/Au films [1], MgO/Heusler alloys [2], and Gd/Cr multilayers, mainly by means of the X-ray magnetic circular dichroism (XMCD) technique. In addition, a polarized neutron reflectivity apparatus is being constructed at J-PARC, which will be a powerful tool for investigating magnetic thin films and multilayers. We also plan to perform muon spin rotation experiments using ultra-slow muon sources.

4-2 Facility: A new XMCD apparatus with 1.2 T magnetic field

A new XMCD apparatus equipped with a water-cooled 1.2-T electromagnet and a liquid N₂ or He cryostat has been developed at BL-16A of the Photon Factory, in order to facilitate XMCD measurements (Fig. 1). Both of the total electron yield and total fluorescence yield modes are available. Samples can be cooled down to below 40 and 100 K, by using liquid He and N₂, respectively. The magnetic field can be switched at each photon energy in order to improve the data quality.

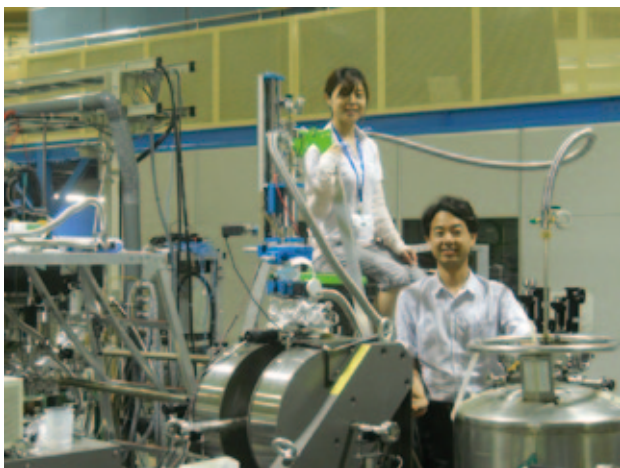


Fig. 1 New XMCD apparatus with a 1.2-T magnet.

4-3 Experimental technique: Development of polarization switching

The fast polarization switching technique in the soft X-ray region is being developed at BL-16A of the Photon Factory, with support from the “Quantum Beam Technology Program” of MEXT. Two tandem APPLE-II type undulators are set to different polarizations, and the switching is realized by modulating the electron orbit through the undulators. Commissioning is still under way, but the quality of the XMCD data has been significantly improved, as shown in Fig. 2. Such a technique is essential to detect small XMCD signals from the surface and interface. Moreover, we plan to combine this technique with the depth-resolved XMCD measurements, in which the surface and interface components can be separated from the bulk contribution. A multi-anode microchannel plate detector is being developed to realize this novel technique.

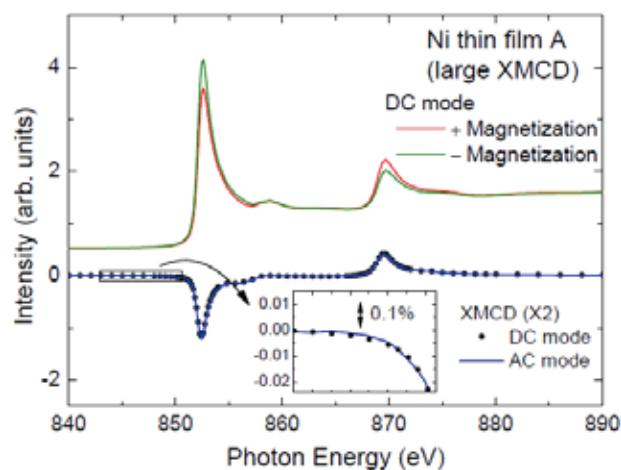


Fig. 2 Ni L-edge XMCD spectra taken by reversing the magnetic field before each measurement (DC mode) and by adopting polarization switching (AC mode).

4-4 Scientific Topics (1): Formation of a NiO-like single layer on Ni/Cu(001) [3, 4]

Much effort has been made in the last decade to fabricate and investigate the interface between ferromagnetic (FM) and antiferromagnetic (AFM) materials, owing to their fascinating magnetic properties such as exchange bias and uncompensated spin at the interface. The magnetic coupling at the FM/AFM interface is key to the appearance of such interesting phenomena. A sharp interface can hardly be obtained, however, by just growing FM and/or AFM thin films, due to some difficulties such as lattice mismatch and intermixing. On the other hand, it seems a reasonable idea to fabricate an AFM transition metal oxide such as NiO on a FM transition metal thin film by oxidizing only the surface of the metal film. With this

approach, however, the degree of oxidation should be carefully controlled.

Another possibility for fabricating a sharp FM/AFM interface can be found in the literature [5], though such a procedure was originally established for a different purpose. A Cu(001) substrate is first covered with atomic oxygen and then a Ni film is grown on the oxygen-covered surface as illustrated in Fig. 3. The amount of oxygen is limited to the saturation coverage on Cu(001), and more importantly, the oxygen atoms always stay at the surface during the Ni deposition, resulting in O/Ni/Cu(001). The thickness of the Ni oxide layer is thus limited to 1 ML, leading to a sharp FM/AFM interface. Moreover, the layer-by-layer growth mode is enhanced by the presence of the oxygen atoms, which act as a surfactant. A question arises, however, whether the surface Ni layer covered with oxygen can be regarded as NiO. Therefore, we used the depth-resolved X-ray absorption spectroscopy (XAS) technique [6] combined with linear and circular polarizations, in order to clarify the chemical state and magnetic structure of the surface layer.

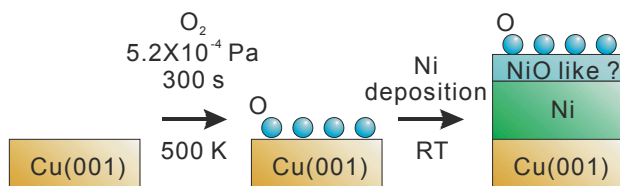


Fig. 3 Schematic diagram of the preparation of O/Ni/Cu(001).

The sample was mounted with [110] lying in the horizontal plane, which is the magnetic easy axis of the present Ni films as illustrated in Fig. 4. A pulsed magnetic field of ~ 500 Oe, which is parallel to the incident X-ray beam, was applied for 1 s before each measurement. The horizontal and vertical linear polarizations, E_h and E_v , were used in the normal incidence (NI) configuration in order to make the electric vector, E , parallel ($E//x$) and perpendicular ($E//y$) to the magnetization direction, respectively. In addition, the combination of E_h and the grazing incidence (GI) configuration was adopted to make the electric vector nearly parallel to the surface normal direction, z , denoted as $E//z$. The depth-resolved XMCD measurements were also performed in the same layout as shown in Fig. 4, by using the circularly polarized X-rays.

Figure 5(a) shows XAS data taken at three different probing depths, λ_e , of 0.6, 0.8 and 1.0 nm. All the spectra show basically the same feature, but one can find a decrease in the satellite feature appearing at 6-eV higher photon energy than the L_3 main peak

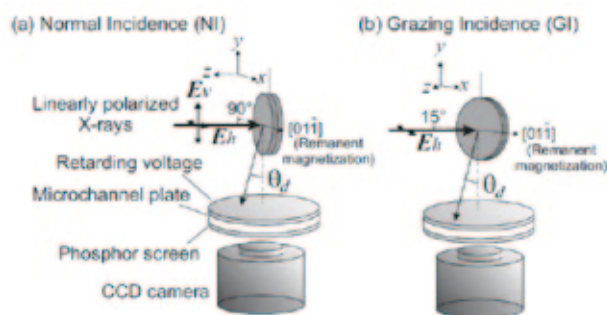


Fig. 4 Schematic layout of the depth-resolved XAS measurement in (a) normal and (b) grazing X-ray incidence configurations.

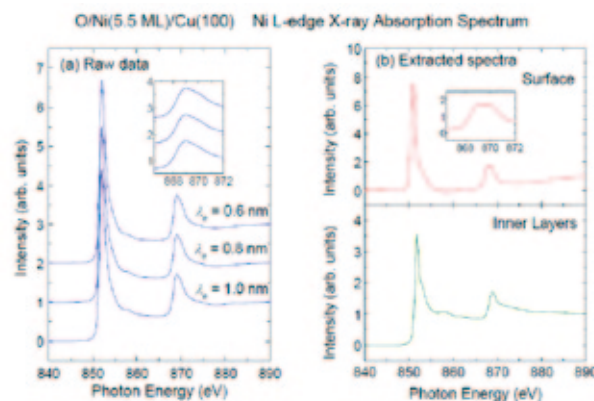


Fig. 5 (a) Ni L-edge XAS taken at different probing depths and (b) extracted surface and inner-layer components.

(~ 852 eV) with decreasing λ_e , i.e. increasing surface sensitivity. Moreover, a shoulder structure at the higher energy side of the L_2 peak (~ 870 eV) becomes more prominent in a more surface-sensitive spectrum.

Next, we extracted the surface and inner-layer components of the XAS spectrum from a set of data with different λ_e . In the extraction process, the Ni film was divided into two regions, the surface layer with a 1 ML thickness and the underlying inner layers, and it was assumed that each layer in the inner layers shows the same X-ray absorption spectrum. The surface and inner-layer components were determined so as to reproduce the observed spectra with different λ_e by the superposition of two components with proper spectral weights depending on λ_e . The extracted spectra are shown in Fig. 5(b). The surface component exhibits characteristic spectral features of NiO, indicating that a NiO-like layer is formed at the surface of the Ni film. On the other hand, the inner-layer component looks like a typical metallic Ni film spectrum, suggesting that oxidation does not proceed into the inner Ni layers, which is reasonable because the oxygen atoms always stay at the surface [5].

X-ray magnetic linear dichroism (XMLD) measurements were performed, since some antiferromagnetic order is expected in the NiO-like layer. The extracted surface XAS spectra with three electric vectors are plotted in Fig. 6. Since the x and y axes are equivalent considering the four-fold symmetry of the (001) surface except for the magnetic structures, the linear dichroism between the $\mathbf{E} \parallel x$ and $\mathbf{E} \parallel y$ configurations is sensitive to the spin direction of the NiO-like layer. No significant difference is found, however, indicating that the spin moment is not aligned in either the x or y direction.

On the other hand, small peak shifts are found between the in-plane, $\mathbf{E} \parallel x$ and $\mathbf{E} \parallel y$, and the out-of-plane, $\mathbf{E} \parallel \sim z$, configurations. This dichroic behavior is consistent with the linear dichroism, which is not attributed to the antiferromagnetic order but to the crystal-field effect due to the low symmetry of the 1-ML NiO-like layer. Therefore, we conclude that no clear magnetic order can be detected in the NiO-like layer, at least in the three primitive directions, x , y , and z .

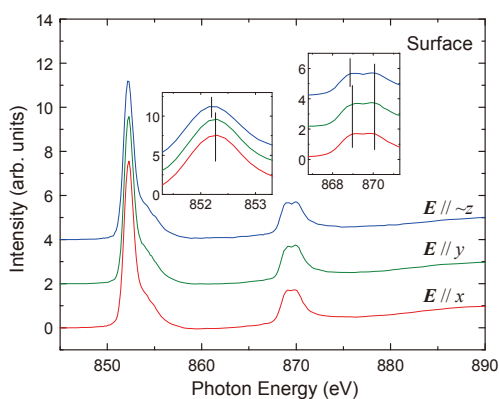


Fig. 6 Extracted surface component of the Ni L-edge XAS spectrum for $\mathbf{E} \parallel x$, $\mathbf{E} \parallel y$, and $\mathbf{E} \parallel \sim z$ configurations.

Finally, the extracted surface and inner-layer components of the XMCD spectrum are shown in Fig. 7, together with the effective spin, m_s^{eff} , and orbital, m_l , magnetic moments estimated by using the XMCD sum rules. The inner layers exhibit typical spectra for Ni metal films, and the estimated magnetic moments are similar to those for bulk Ni. In contrast, the XMCD spectrum for the surface layer exhibits the opposite sign to that for the inner layers, suggesting an antiparallel magnetic coupling between the NiO-like layer and the ferromagnetic Ni layers.

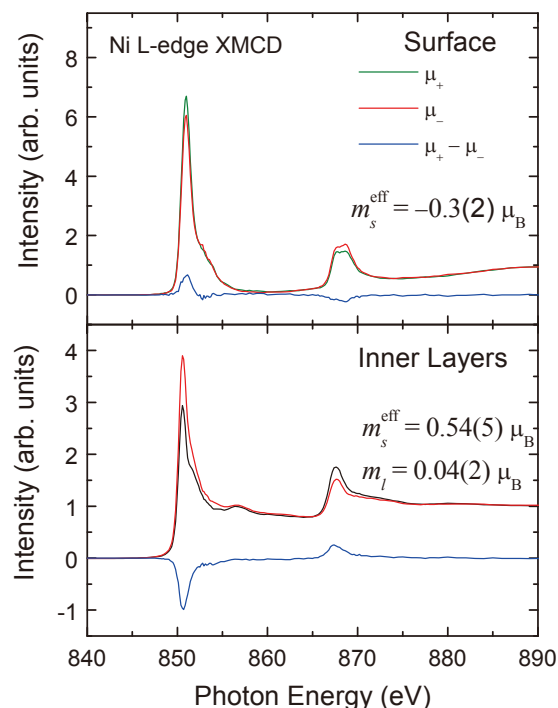


Fig. 7 Extracted surface and inner-layer XMCD components, together with the estimated effective spin, m_s^{eff} , and orbital, m_l , magnetic moments.

4-5 Scientific Topics (2): Element-specific magnetic anisotropy energy of $L1_0$ -type FeNi films

The $L1_0$ -type FeNi multilayer has attracted much attention as a candidate material for rare metal-free perpendicularly-magnetized films for high-density recording media. The $L1_0$ -ordered structure consists of alternate stacking of two different atomic planes along the fcc [001] direction. Therefore, some efforts have been made to achieve perpendicular magnetic anisotropy (PMA) by using alternate monatomic layer deposition on fcc (001) substrates. Although the magnetic properties of the multilayer have been investigated after the deposition of the whole film so far, an *in-situ* analysis of each growth process is also important for understanding the fundamental magnetic properties. In fact, a strong PMA of surface 1 ML Fe on Ni(6–16 ML)/Cu(001) has been reported [7]. This suggests that 1 ML Fe carries the PMA in $L1_0$ -type FeNi, which has a 1 ML Fe layer adjacent to Ni. However, $L1_0$ -type FeNi is composed of the buried Fe and Ni layers, whose magnetic anisotropy energies (MAEs) would be different from that of the surface layer, and therefore it is necessary to investigate, element specifically, the MAEs of sandwiched layers to clarify the origin of the MAE of the whole film. In the present study, we applied *in-situ* XMCD to the alternately-layered FeNi thin films in order to separately estimate the MAEs of Fe and Ni.

A Cu(001) single crystal was cleaned by repeated cycles of Ar⁺ sputtering at 1.5 keV and subsequent annealing at ~900 K. The Ni and Fe layers were then grown at room temperature by the electron bombardment evaporation of Ni and Fe rods. The growth rate of the film was determined by monitoring the oscillatory intensity of a reflection high-energy electron diffraction spot. The Fe and Ni layers were alternately grown on a wedged-shaped Ni(4–20 ML)/Cu(001) substrate. Ni films on Cu(001) are known to show the spin reorientation transition from in-plane to perpendicular directions at the thickness of 7–11 ML. Polar magneto-optic Kerr effect (MOKE) hysteresis curves were measured at room temperature by reflecting a laser beam with $\lambda = 635$ nm off the surface of the samples placed in the center of a yoke coil. XMCD spectra were measured at room temperature by using circularly polarized X-rays. The sample was mounted with [110] lying in the horizontal plane, which is the magnetic easy axis of the in-plane magnetized films. The normal and grazing X-ray incidence geometries were adopted, and denoted as NI and GI. Fe *L*-edge XMCD was measured in the total electron yield mode, whereas the depth-resolved XMCD technique was adopted at the Ni *L* edge in order to eliminate the signal from substrate Ni.

Figure 8 shows polar MOKE hysteresis curves for *n* ML FeNi thin films grown on Ni(10 ML)/Cu(001). A square hysteresis loop is observed for 2 ML film, indicating that the film has PMA. This seems reasonable because the bare Ni(10 ML)/Cu(001) film shows strong PMA. As the FeNi thickness increases, Ni-terminated films, *i.e.* *n* = even, turn to in-plane magnetization. On the other hand, Fe-terminated films keep perpendicular magnetization up to *n* = 5 which diminishes at *n* = 7. This might be due to the strong positive MAE of the surface Fe layer, but element-specific MAE analysis using XMCD is necessary to explain such a complicated behavior of magnetic anisotropy.

Figure 9 shows Fe *L*-edge XMCD spectra for a 4 ML FeNi thin film taken in the total electron yield mode. The films at the substrate Ni thickness *x* = 15 and 5 ML show perpendicular and in-plane magnetization, respectively. The spectral features are almost the same, indicating that the orbital moment difference, Δm_l , between the perpendicular and in-plane magnetization is expected to be small. In fact, the obtained m_l / m_s^{eff} (Fe) is 0.085 and 0.081 for the perpendicularly and in-plane magnetized films, respectively. This directly suggests that the Ni-sandwiched Fe layer does not have a large MAE. In fact, these values lead to MAE of Fe, $K_{\text{Fe}} = 10 \pm 40$ $\mu\text{eV}/\text{atom}$. As opposed to the surface Fe layer on

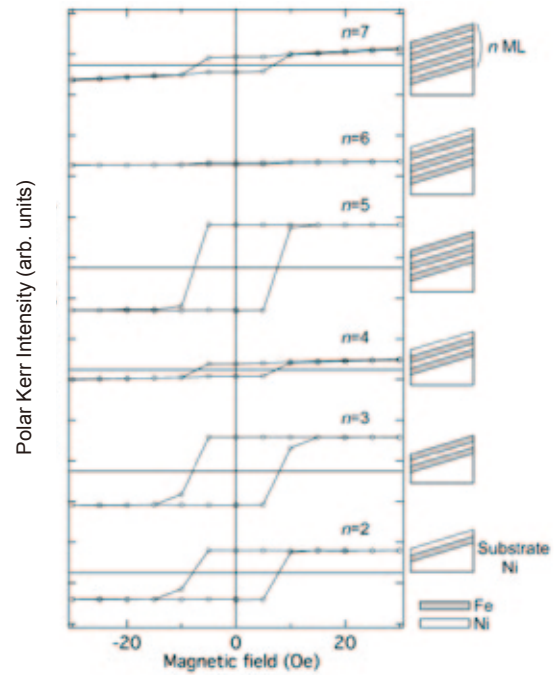


Fig. 8 Polar MOKE hysteresis curves for *n* ML FeNi thin films grown on Ni(10 ML)/Cu(001).

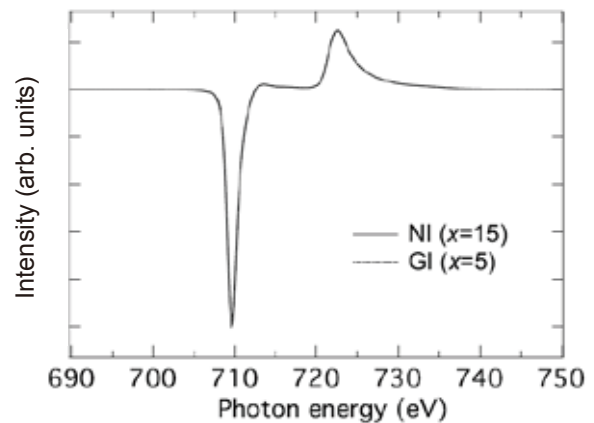


Fig. 9 Fe *L*-edge XMCD spectra for 4 ML FeNi thin film grown on Ni(*x* ML)/Cu(001). The films at *x* = 15 and 5 ML show perpendicular and in-plane magnetization, respectively, and were measured at NI and GI. The spectra are normalized at the *L*₂ peak.

Ni/Cu(001), which shows a large positive MAE of $K_{\text{Fe}}^{\text{S}} = 140 \pm 60$ $\mu\text{eV}/\text{atom}$ [7], the Ni-sandwiched Fe layer almost loses PMA. The MAE of the Fe-sandwiched Ni layer is similarly estimated as $K_{\text{Ni}} = 60 \pm 30$ $\mu\text{eV}/\text{atom}$. As opposed to the surface Ni layer on Cu(001), which shows negative MAE of -180 ± 30 $\mu\text{eV}/\text{atom}$, the Fe-sandwiched Ni layer has a small positive MAE.

Finally, we calculate the total MAE, K_{eff} , of FeNi(*n* ML)/Ni(*x* ML)/Cu(001) films by using the obtained MAEs of sandwiched Fe and Ni layers, K_{Fe} and K_{Ni} . In addition, the MAE of the top Ni layer of substrate Ni,

$K_{\text{Ni}}^{\text{top}} = -34 \pm 15 \mu\text{eV}/\text{atom}$, the bulk MAE component of substrate Ni, $K_{\text{V}} = 34 \pm 15 \mu\text{eV}/\text{atom}$, and the MAE of surface Fe, $K_{\text{Fe}}^{\text{S}} = 140 \pm 60 \mu\text{eV}/\text{atom}$, are taken from the literature [7]. The surface Ni contribution, K_{Ni}^{S} , is found to be $-30 \pm 20 \mu\text{eV}/\text{atom}$ by depth-resolved XMCD analysis using the 2 ML FeNi films. Figure 10 shows the total MAE, $K_{\text{eff}} t$, of FeNi(n ML)/Ni(x ML)/Cu(001), which shows good agreement with the polar MOKE result, indicating that the element-specific MAEs obtained from XMCD are reliable.

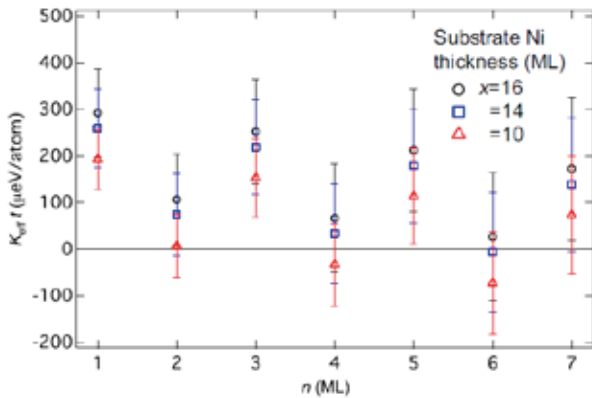


Fig. 10 $K_{\text{eff}} t$ of FeNi(n ML)/Ni(x ML)/Cu(001) simulated by using MAEs obtained from XMCD analysis. The substrate Ni thicknesses of 10, 14 and 16 ML are adopted.

- [1] M. Sakamaki and K. Amemiya, J. Phys.: Conf. Ser. **266** (2011) 012020.
- [2] D. Asakura et al., Phys. Rev. B **82** (2010) 184419.
- [3] K. Amemiya and M. Sakamaki, Appl. Phys. Lett. **98** (2011) 012501.
- [4] K. Amemiya and M. Sakamaki, J. Phys. D **44** (2011) 064018.
- [5] R. Nünthel, et al., Surf. Sci. **531** (2003) 53.
- [6] K. Amemiya et al., Appl. Phys. Lett. **84** (2004) 936.
- [7] H. Abe et al., J. Magn. Magn. Mater. **302** (2006) 86.